

The 8th International Electronic Conference on Medicinal Chemistry (ECMC 2022)

01–30 NOVEMBER 2022 | ONLINE

In silico investigations of dihydrophenanthrene derivatives as potential inhibitors of SARS-CoV-2

Chaired by **DR. ALFREDO BERZAL-HERRANZ**;
Co-Chaired by **PROF. DR. MARIA EMÍLIA SOUSA**



pharmaceuticals



**Imane Yamari¹, Suraj N. Mali², Oussama Abchir¹, Hassan Nour¹,
Said Gmouh³, M'Hammed El Kouali¹, Samir Chtita^(1,*)**

1 Laboratory of analytical and molecular chemistry, Faculty of sciences Ben M'Sik, Hassan II university of Casablanca, B.P 7955, Casablanca, Morocco;

2 Department of pharmaceutical sciences & technology, Birla institute of technology, Mesra, Ranchi, India;

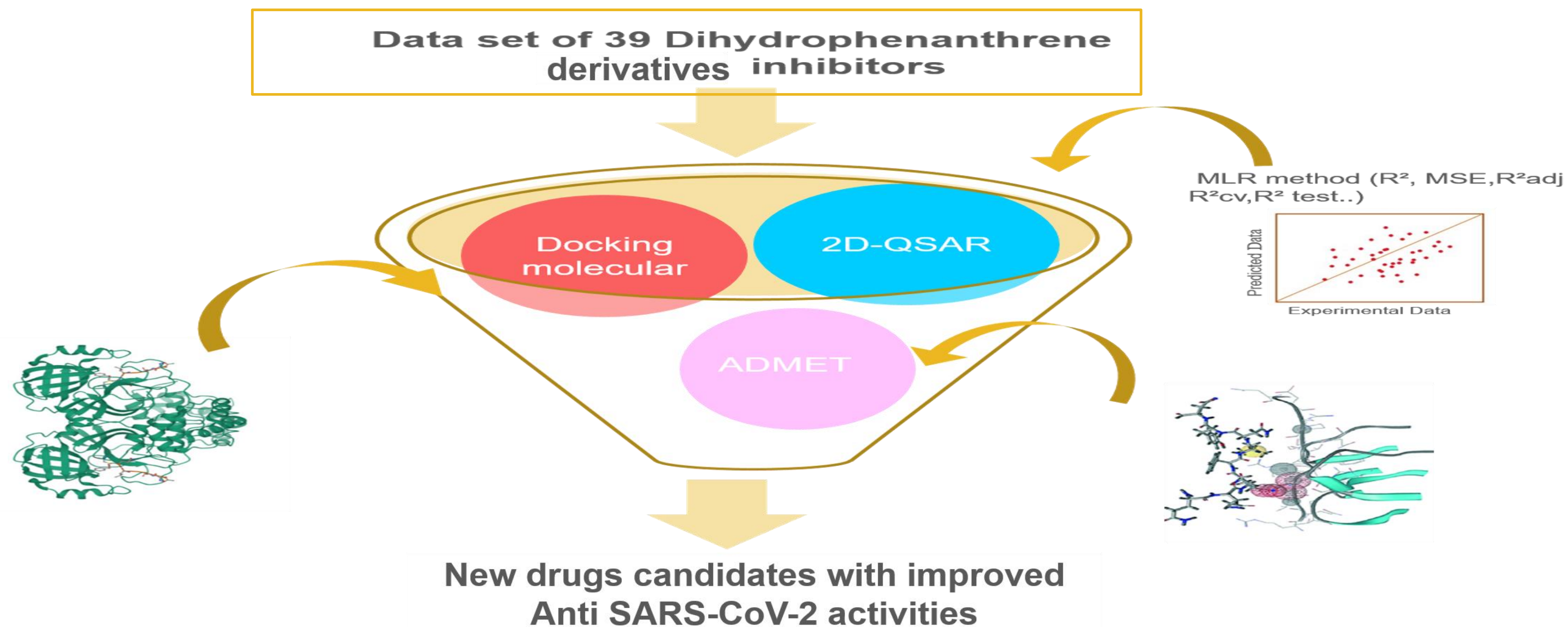
3 Laboratory LIMAT, Faculty of Sciences Ben M'Sik, Hassan II University of Casablanca, B.P 5366 Maarif, Casablanca, Morocco.

* Corresponding author: samirchtita@gmail.com



In silico investigations of 9,10 dihydrophenanthrene derivatives as potential inhibitors of SARS-CoV-2

Graphical abstract



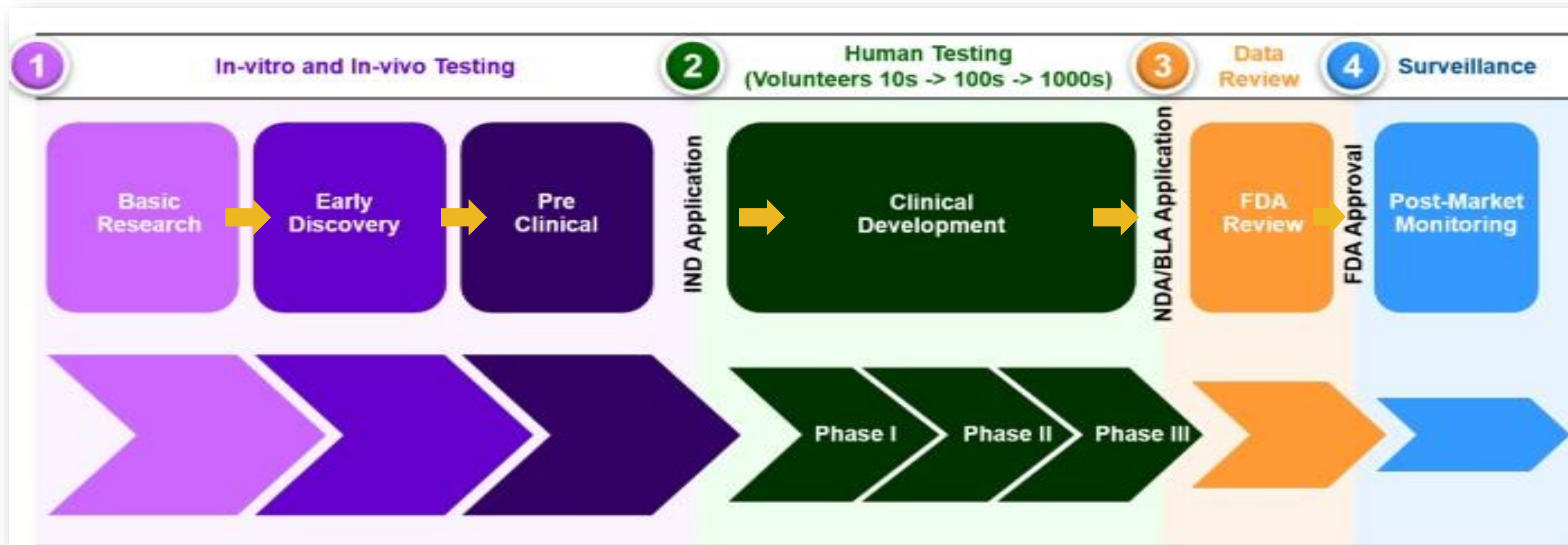
Abstract

Since its appearance in Wuhan on December 2019, finding ways to manage the COVID19 pandemic becomes the biggest challenge the world is facing. In this investigation, we used quantitative structure-activity relationship (QSAR) study, Absorption, distribution, metabolism, excretion, and toxicity (ADMET) analysis and computational molecular docking simulations to screen and assess the efficacy of thirty-nine bioactive 9,10-dihydrophenanthrene analogues. The density functional theory (DFT) optimization using the B3LYP/6-31G(d, p) level was used for the calculations of molecular descriptors and the principal component analysis (PCA) was used to eliminated redundant and non-significant descriptors. After that, statistically robust models were developed using multiple linear regression (MLR) method. All derived models were then subjected to thorough external as well as internal statistical validations, Y-randomization and applicability domain analysis. These validations were carried out as per the OECD principles. The best built model was used to design new molecules that have good inhibitory activity against SARS-CoV-2. Pharmacokinetics properties were then determined using ADMET analysis to weed out any that would be harmful to the human body or cause adverse effects. Through the use of computational molecular docking simulations, in silico research was conducted on deigned compounds to forecast their SARS-CoV-2 activity and determine the stability of the evaluated ligands during their contacts with the protein of desired activity.

Keywords: SARS-CoV-2, Dihydrophenanthrene, QSAR, MLR, ADMET, Molecular Docking.



Introduction



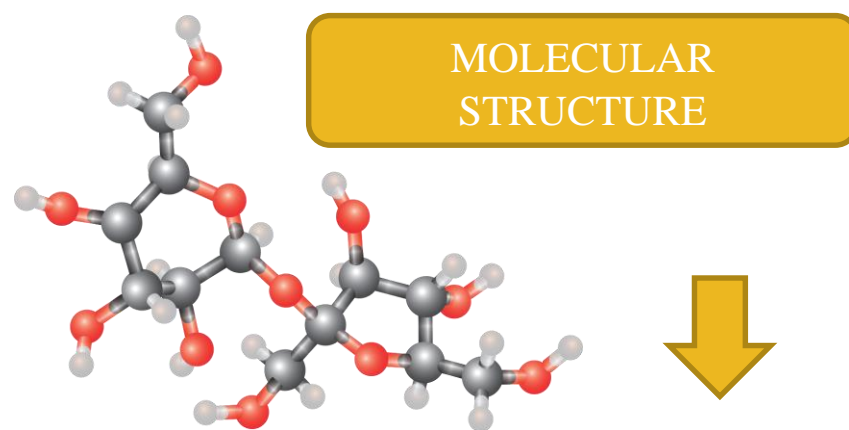
Experiences

Money

Time



2D-QSAR methodology and validation



$$\text{Activity} = f(\text{Molecular Descriptors})$$

ACTIVITY PREDICTION FOR NEW MOLECULES

DESCRIPTORS CALCULATION

DESCRIPTIVE STATISTICS

MODEL GENERATION : QSAR

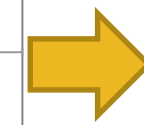
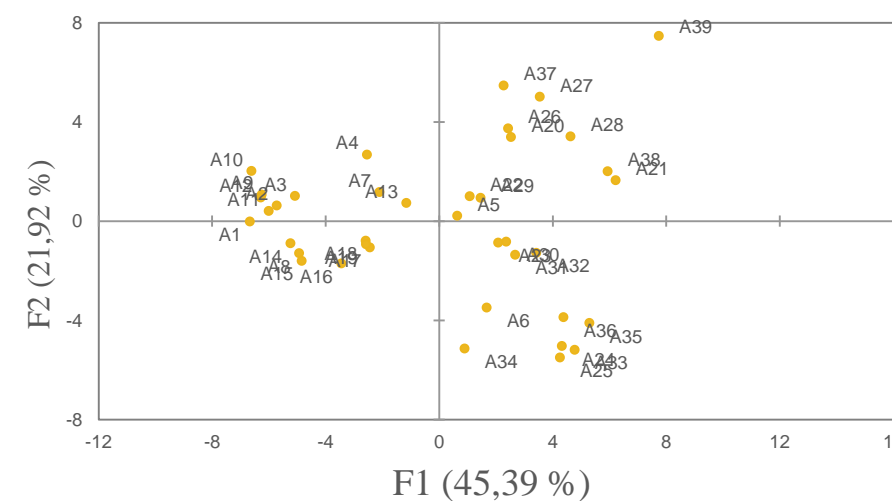
VALIDATION OF THE MODEL

Symbol	Name and description	Nature ^a	Origin ^b	Ref. ^c
M_r	Relative molecular mass	steric	compos	tw
I_x	First principal moment of inertia (around axis X)	steric	comput	tw
I_y	Second principal moment of inertia (around axis Y)	steric	comput	tw
I_z	Third principal moment of inertia (around axis Z)	steric	comput	tw
I_{xy}	Ratio between the principal moments $I_x I_y$	steric	comput	tw
I_{yz}	Ratio between the principal moments $I_y I_z$	steric	comput	tw
I_{xz}	Ratio between the principal moments $I_x I_z$	steric	comput	tw
S_x	Molecular area projected on the YZ plane (along X axis, in the CPK molecular model)	steric	molgrp	tw
S_y	Ratio between the area S_x and the area of the YZ face of the molecular box defined by the farthest CPK spheres (in the CPK molecular model), expressed as %	steric	molgrp	tw
α	Molecular polarizability	electron	comput	tw
$ \beta $	Absolute second-order molecular polarizability β	electron	comput	tw
$ \beta_x $	Absolute X component of β	electron	comput	tw
γ	Third-order molecular polarizability	electron	comput	tw
D_x	X component of molecular dipole moment	electron	comput	pw, tw
D_y	Y component of molecular dipole moment	electron	comput	pw, tw
D_z	Z component of molecular dipole moment	electron	comput	pw, tw
n_s	Surface molecular density projected on the YZ plane, defined as N/S_x , where N is the number of atoms	steric	comput	tw
Δ_1	The length of the molecular box along the axis X (in the CPK molecular model)	steric	molgrp	tw
Δ_{12}	The width/height/depth ratio of the YZ face of the molecular box (in the CPK molecular model)	steric	molgrp	tw
W_{max}	Maximum of X coordinate $\pm r dW$ radius)	steric	comput	tw
W_{min}	Difference between the maximum and minimum of X coordinate $\pm r dW$ radius)	steric	comput	tw
W_{xy}	Ratio between the W_{x1} and W_{x2} differences	steric	comput	tw
A_{xy}	Area of the XY face of the molecular box defined by the minimum and maximum atomic coordinates	steric	comput	tw
A_{yz}	Area of the YZ face of the molecular box defined by the minimum and maximum atomic coordinates	steric	comput	tw
A_{xz}	Area of the molecular box defined by the minimum and maximum atomic coordinates	steric	comput	tw
Δ_{xy}	Ratio between the X and Y edges of the molecular box defined by the minimum and maximum atomic coordinates	steric	comput	tw
Δ_{yz}	Ratio between the Y and Z edges of the molecular box defined by the minimum and maximum atomic coordinates	steric	comput	tw
Δ_{xz}	Ratio between the X and Z edges of the molecular box defined by the minimum and maximum atomic coordinates	steric	comput	tw

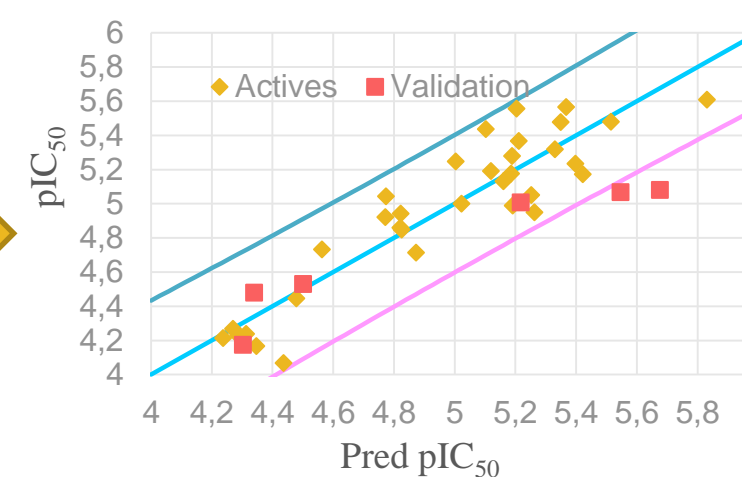
pIC₅₀



Observations (axes F1 et F2 : 67,31 %)



Pred pIC₅₀ / pIC₅₀



X= Molecular descriptors

Y=Experiments assay (Activity)

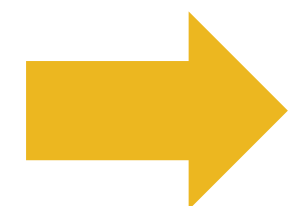
Principal Component Analysis (PCA)

Multiple linear regression (MLR)

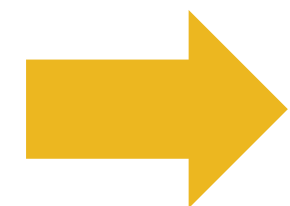
- Statistical tests
- Internal and external validations
- Applicability Domain AD



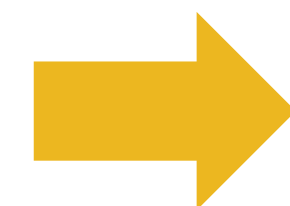
Pharmacokinetic properties



A good activity while using the QSAR methods



A good selectivity and affinity to the target in the results of the molecular docking and the molecular dynamics studies .



A good pharmacokinetic profile:
the Absorption, Distribution, Metabolism, Excretion
and Toxicity (ADMET) properties must be checked.



SARS-CoV-2

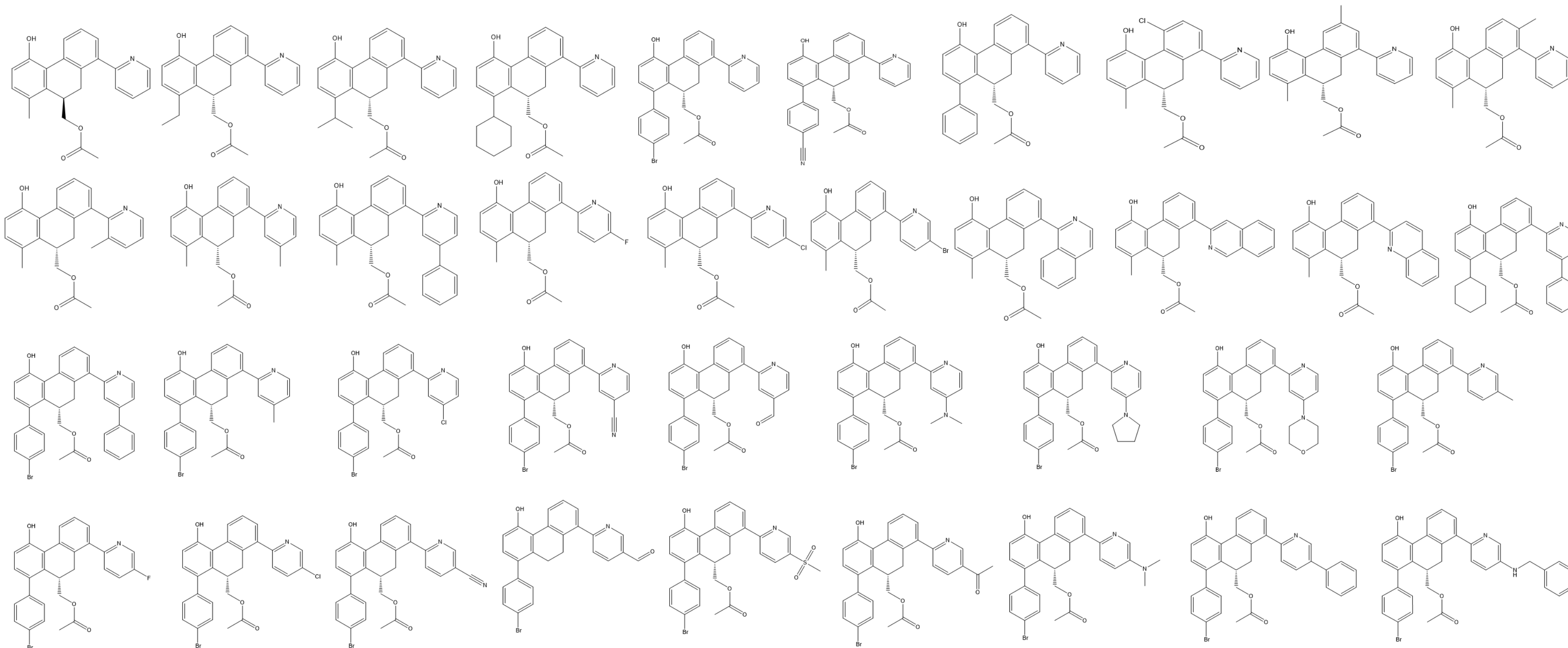
At the end of 2019, a cluster of pneumonia cases occurred in Wuhan, China. It then quickly spread to other parts of the world causing a pandemic situation popularly termed as Coronavirus (CoV) Disease-2019 (COVID19).

With the aim of prioritizing the candidate drugs, various chem-bioinformatics methods were used. According to the study of Jian-Wei Zhang and al (2022) , the discovery of non-covalent SARS-CoV-2, 3CLpro inhibitors (9,10-dihydrophenanthrene scaffold) was with fluorescence resonance energy transfer (FRET) biochemical assay. Also, the in vitro metabolic stability in the gastrointestinal tract, human plasma, and liver microsome, were validated. So we based our work, on the dataset established by the previous study of thirty-nine (39) substituted 9, 10-dihydrophenanthrene analogs covering a wide chemical space and having moderate to high activity against the COVID-19 virus strain.



Application

2D-QSAR study of 9,10 dihydrophenanthrene derivatives as potential inhibitors of SARS-CoV-2



Molecular descriptors

Chem3D



- Molecular Weight
- Number of HBond Acceptors
- Number of HBond Donors
- Molecular Refractivity
- Coefficient of partition Octanol/Water
- Pka (log units)
- Number Rotatable Bonds
- Polar Surface Area
- Topological Diameter

Gaussian 09

DFT (B3LYP, 6-31G(d))



- Energy gap
- Dipole Moment
- Electronegativity
- Energy gap
- Energy HOMO
- Energy LUMO



Molecular descriptors

PaDEL and ChemDes



- AATS5e
- MATS2m
- VE3_DzZ
- SpMin2_Bhi
- RDF145m
- Nacc
- Nrot
- Moment dipolar
- Weight
- Energy HOMO
- Energy LUMO



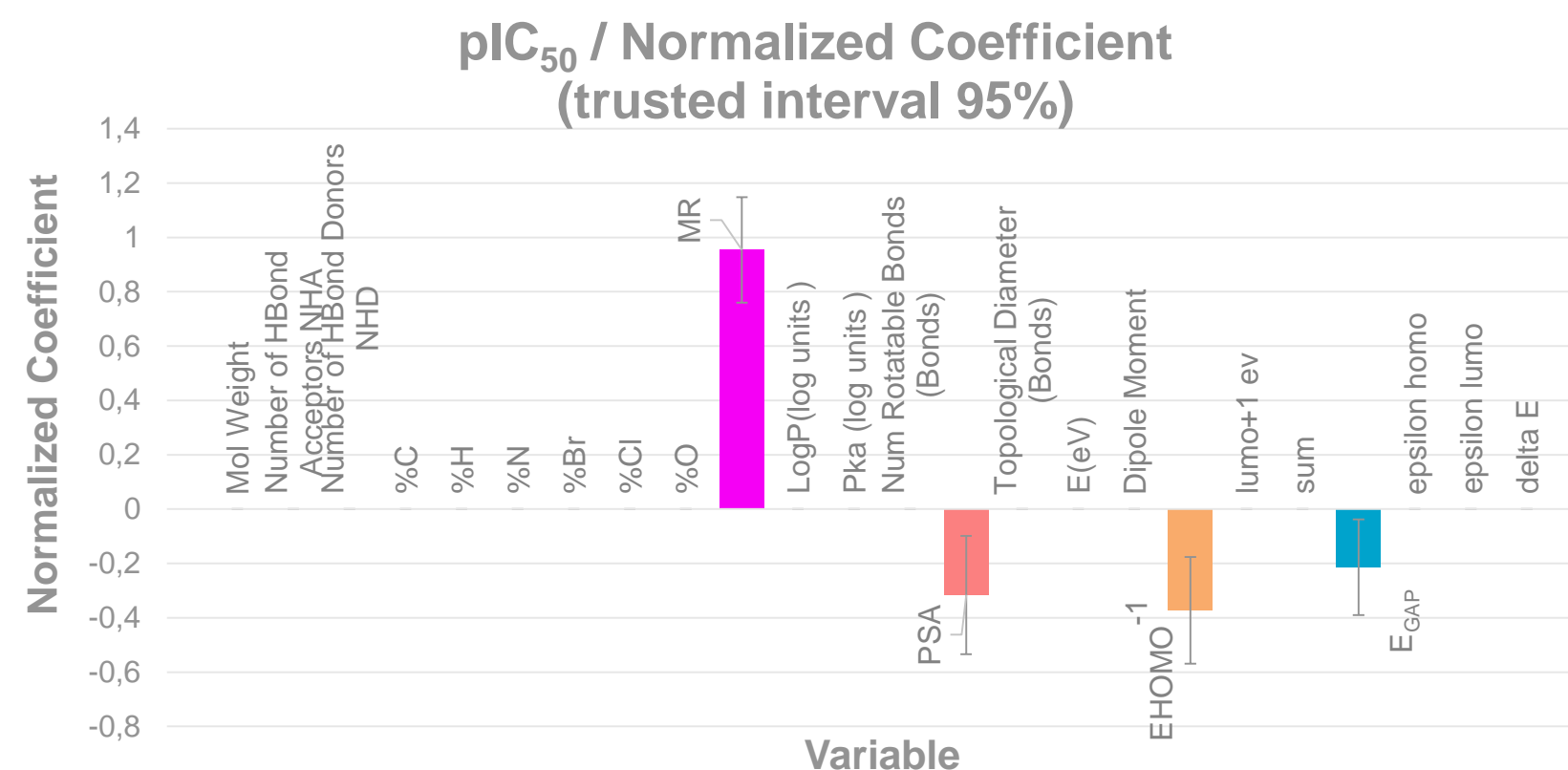
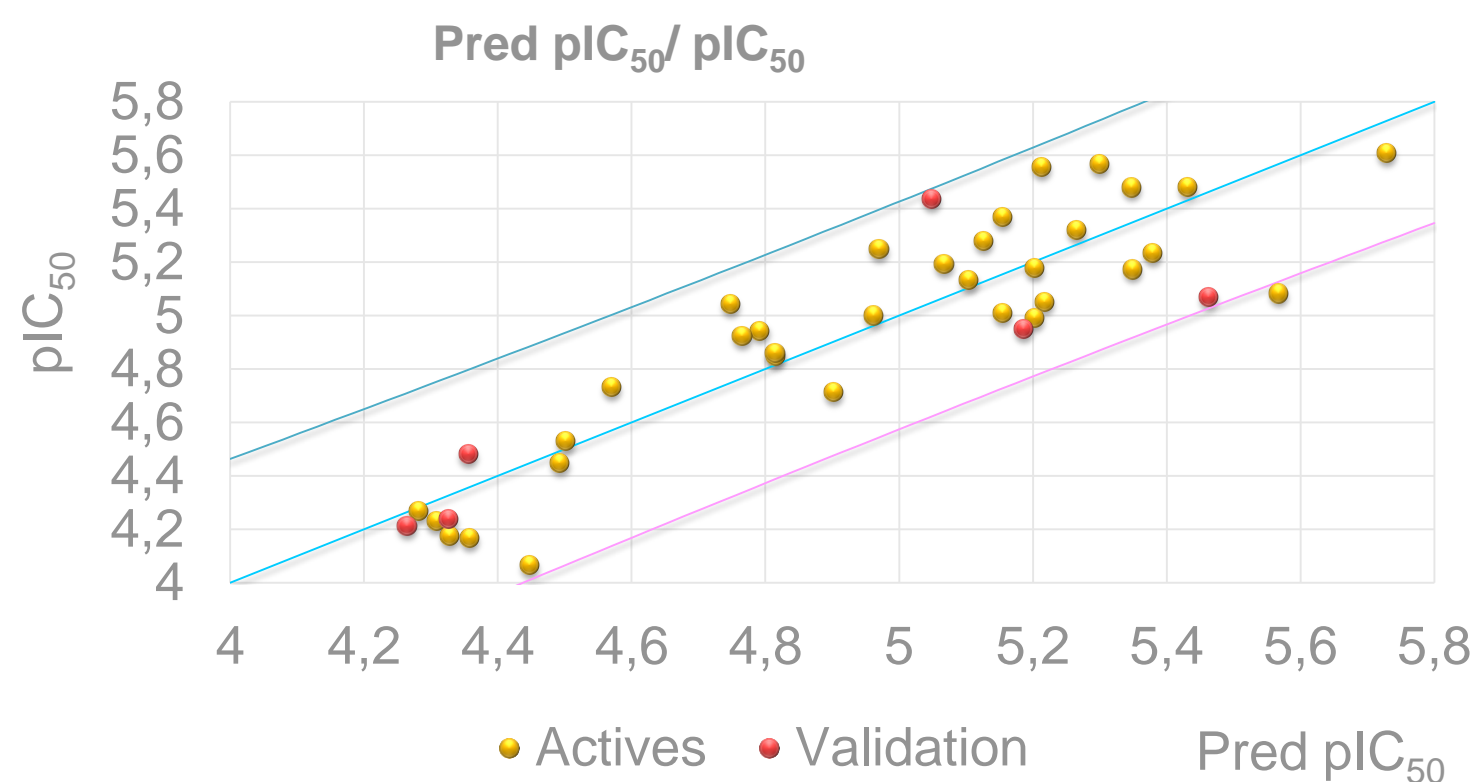
Results and discussion

$$\text{pIC}_{50} = f(\text{MR}, \text{PSA}, E_{\text{GAP}}, E_{\text{Homo-1}})$$

$R^2 = 0.805$ $R^2_{\text{adj}} = 0.777$ $R^2_{\text{cv}} = 0.732$ $R^2_{\text{test}} = 0.731$ $\text{MSE} = 0.042$ $F = 28.951$ $P \text{ value} < 10^{-4}$

$$\text{pIC}_{50} = f(\text{AATS5e}, \text{MATS2m}, \text{VE3_DzZ}, \text{SpMin2_Bhi}, \text{RDF145m})$$

$R^2 = 0.895$ $R^2_{\text{adj}} = 0.872$ $R^2_{\text{cv}} = 0.855$ $\text{MSE} = 0.042$ $F = 39.422$ $P \text{ value} < 10^{-4}$



Statistical parameters for the best MLR model

Statistical parameters

R^2	0.805	>0.600
R^2_{adj}	0.777	>0.600
MSE	0.042	A low value
F	28.951	A high value

Internal validation

R^2_{cv}	0.732	>0.500
Average of 50 R^2_{rand}	0.100	< R^2
Average of 50 $R^2_{cv rand}$	-0.253	< R^2_{cv}
cR^2p	0.758	>0.500

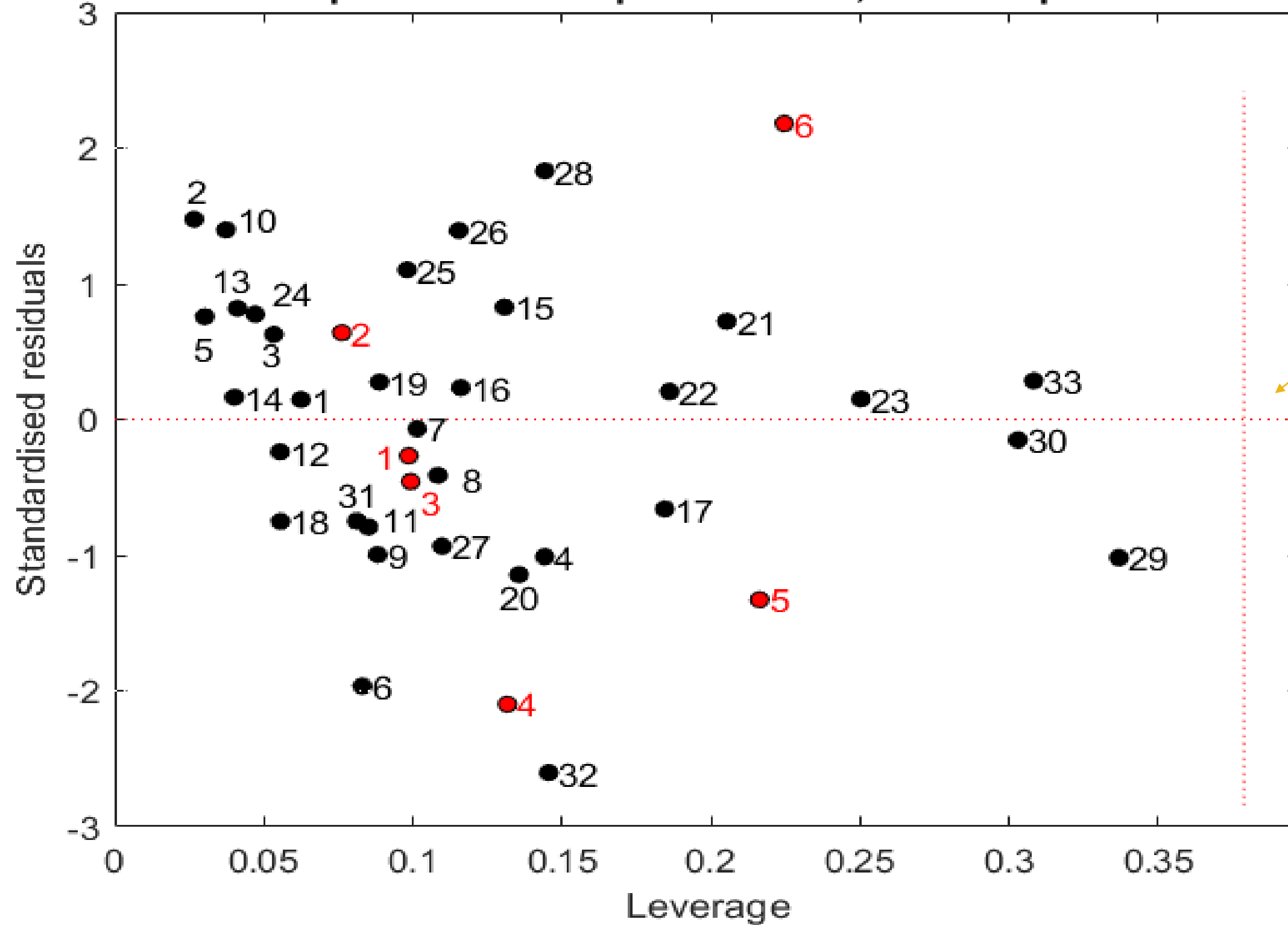
External validation

R^2_{test}	0.731	>0,600
--------------	-------	--------



Applicability Domain (AD)

William plot - train samples in black, test samples in red

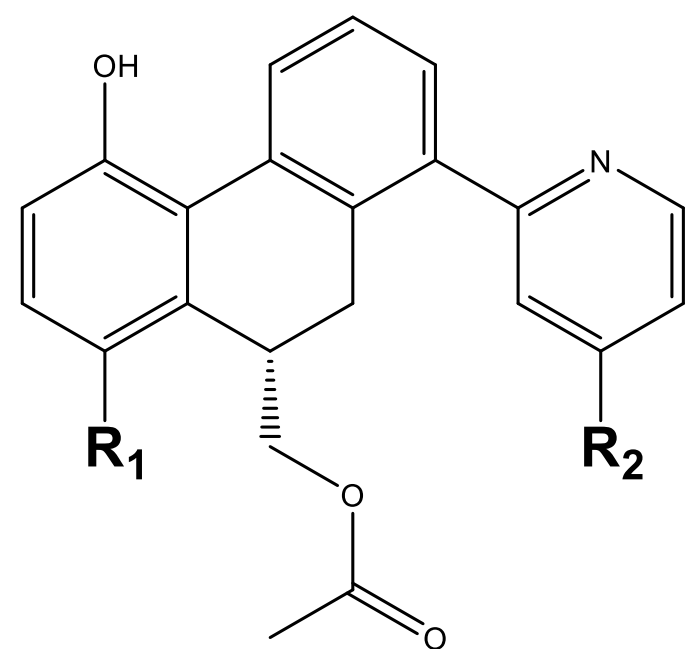


$h^* = 3(k+1)/n = 0,378$

Résidual limits = [+3,- 3]



The new designed molecules



Structures of the proposed molecules proposed by the MLR model based on molecule 21:

$R_1 = 4\text{-Br Phenyl}$ $R_2 = 5\text{-Ph}$

The anti SARS-CoV2 activity values

$pIC_{50}(21) = 5.61$ $h^* = 0.378$

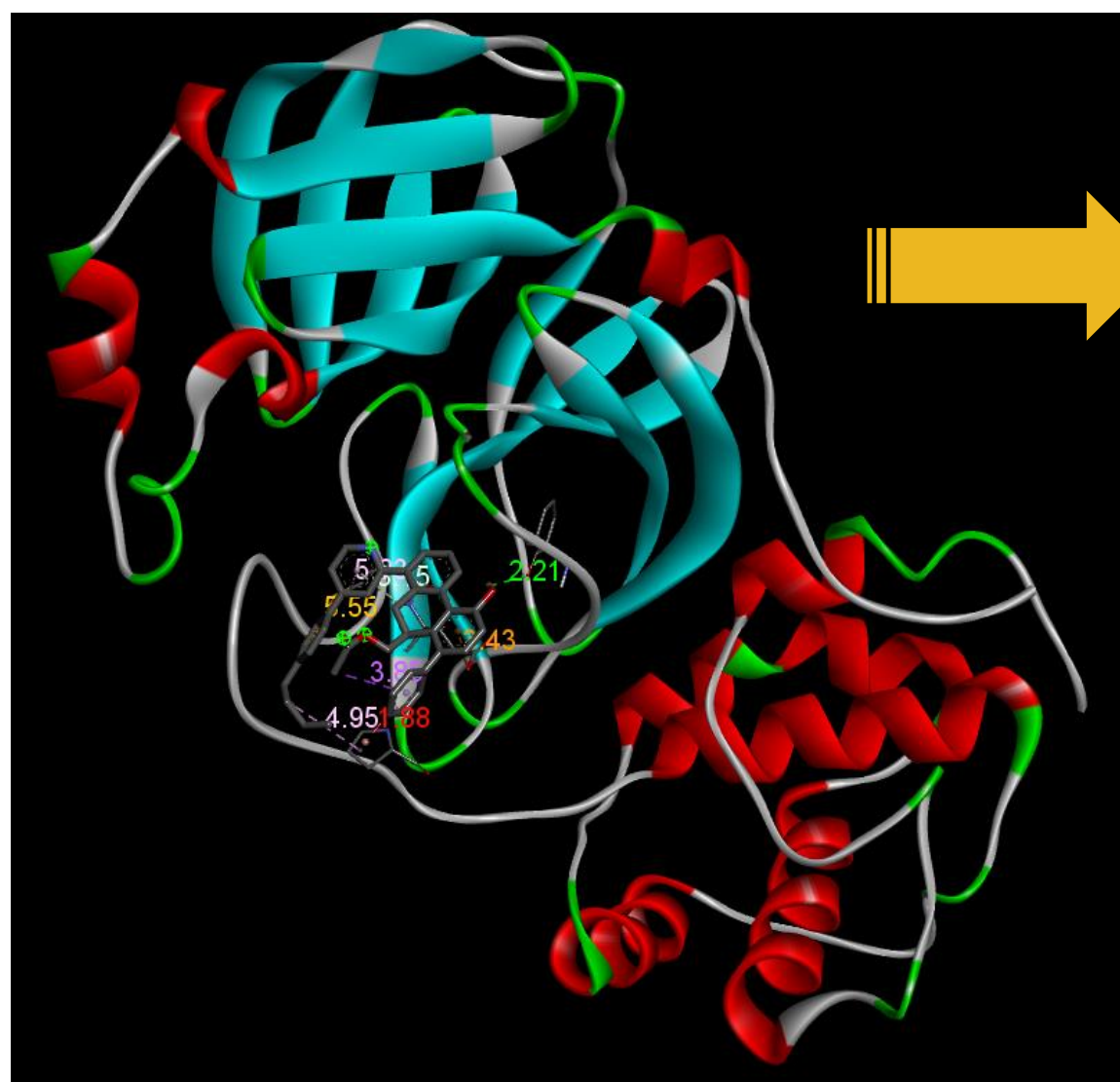


N° Molecules	R_1	R_2	MR	PSA	E_{GAP}	$E_{Homo^{-1}}$	pIC_{50}	h
1			19.278	58.89	0.159	-5.887	6.147	0.494
2			18.202	58.89	0.167	-6.286	6.354	0.316
3			20.832	58.89	0.154	-6.061	6.307	0.709
4			20.055	58.89	0.153	-6.029	6.295	0.595
5			17.711	58.89	0.168	-6.127	6.235	0.291
6			20.260	58.89	0.154	-6.078	6.319	0.618



Molecular docking :

3D Representation of the interaction between the active sites of 6LU7 and ligand 2



	Name	Visible	Color	Parent	Distance	Category	Types
1	A:THR19...	<input type="checkbox"/> No	Green	Ligand No...	2,95755	Hydrogen Bond	Conventional Hydrogen ...
2	A:GLN19...	<input type="checkbox"/> No	Green	Ligand No...	2,9208	Hydrogen Bond	Conventional Hydrogen ...
3	:UNK0:H5...	<input type="checkbox"/> No	Green	Ligand No...	2,66162	Hydrogen Bond	Conventional Hydrogen ...
4	A:MET16...	<input type="checkbox"/> No	Light Green	Ligand No...	3,36287	Hydrogen Bond	Carbon Hydrogen Bond
5	A:HIS41:...	<input checked="" type="checkbox"/> Yes	Orange	Ligand No...	4,92427	Electrostatic	Pi-Cation
6	A:CYS14...	<input type="checkbox"/> No	Light Green	Ligand No...	4,18389	Hydrogen Bond	Pi-Donor Hydrogen Bond
7	A:MET49:...	<input checked="" type="checkbox"/> Yes	Purple	Ligand No...	3,5561	Hydrophobic	Pi-Sigma
8	:UNK0:C2...	<input checked="" type="checkbox"/> Yes	Purple	Ligand No...	3,75776	Hydrophobic	Pi-Sigma
9	:UNK0:CL...	<input checked="" type="checkbox"/> Yes	Purple	Ligand No...	3,84441	Hydrophobic	Pi-Sigma
10	A:CYS14...	<input checked="" type="checkbox"/> Yes	Yellow	Ligand No...	5,99419	Other	Pi-Sulfur
11	:UNK0 - A...	<input checked="" type="checkbox"/> Yes	Pink	Ligand No...	5,41537	Hydrophobic	Pi-Alkyl
12	:UNK0 - A...	<input checked="" type="checkbox"/> Yes	Pink	Ligand No...	4,31248	Hydrophobic	Pi-Alkyl



Molecular docking

3D Representation of the interaction between the active sites of 6LU7 and ligand 5



Name	Visible	Color	Parent	Distance	Category	Types
1 A:THR190:HN - :UNK0:O21	<input type="checkbox"/> No	■	Ligand N...	2,87249	Hydrogen Bond	Conventional Hydrogen Bond
2 A:MET165:CA - :UNK0:N16	<input type="checkbox"/> No	■	Ligand N...	3,35956	Hydrogen Bond	Carbon Hydrogen Bond
3 A:GLN189:CA - :UNK0:O21	<input type="checkbox"/> No	■	Ligand N...	3,44069	Hydrogen Bond	Carbon Hydrogen Bond
4 A:MET49:CE - :UNK0	<input checked="" type="checkbox"/> Yes	■	Ligand N...	3,57554	Hydrophobic	Pi-Sigma
5 :UNK0:C26 - :UNK0	<input checked="" type="checkbox"/> Yes	■	Ligand N...	3,77466	Hydrophobic	Pi-Sigma
6 A:CYS145:SG - :UNK0	<input checked="" type="checkbox"/> Yes	■	Ligand N...	5,95165	Other	Pi-Sulfur
7 :UNK0 - A:PRO168	<input checked="" type="checkbox"/> Yes	■	Ligand N...	5,40178	Hydrophobic	Pi-Alkyl
8 :UNK0 - A:MET165	<input checked="" type="checkbox"/> Yes	■	Ligand N...	4,21981	Hydrophobic	Pi-Alkyl
9 :UNK0 - A:CYS145	<input checked="" type="checkbox"/> Yes	■	Ligand N...	4,99805	Hydrophobic	Pi-Alkyl



Evaluation of drug-likeness properties

Properties	MW	Log P	HBA	HBD	Surface area	RB	Docking score
Rules	<500 Da	<5	<10	<5	<140 A ²		
Molecule 7	632.598	9.763	4	1	261.095	8	-8.4 kcal/mol
Molecule 10	667.043	9.982	4	1	271.398	9	-8.2 kcal/mol



Predicted ADMET properties of the designed compounds

Property	Model Name	Predicted Value for molecule 10	Predicted Value for molecule 7	Unit
Absorption	Intestinal absorption (human)	94.741	95.333	Numeric (% Absorbed)
Distribution	VDss (human)	-1.286	-1.251	Numeric (log L/kg)
Distribution	Fraction unbound (human)	0.337	0.333	Numeric (Fu)
Metabolism	CYP2D6 substrate	No	No	Categorical (Yes/No)
Metabolism	CYP3A4 substrate	Yes	Yes	Categorical (Yes/No)
Metabolism	CYP1A2 inhibitor	Yes	No	Categorical (Yes/No)
Metabolism	CYP2C19 inhibitor	No	No	Categorical (Yes/No)
Metabolism	CYP2C9 inhibitor	Yes	Yes	Categorical (Yes/No)
Metabolism	CYP2D6 inhibitor	No	No	Categorical (Yes/No)
Metabolism	CYP3A4 inhibitor	No	No	Categorical (Yes/No)
Excretion	Total Clearance	-0.213	-0.206	Numeric (log ml/min/kg)
Toxicity	AMES toxicity	No	No	Categorical (Yes/No)



Conclusion

- In this work, we developed MLR-2D QSAR model for a series of 39 dihydrophenanthrene derivatives as potential inhibitors of SARS-CoV-2.
- We designed six molecules based on the best built MLR model,
- Among the molecules designed, two molecules with high activities that belongs to the applicability domain, and both of the molecules respects the ADMET properties.
- These two molecules can be considered as a drug-candidates after conducting additional *in vivo* and *in vitro* investigations before the clinical trial procedure.



THANK YOU!

ECMC
2022

The 8th International Electronic
Conference on Medicinal Chemistry

01-30 NOVEMBER 2022 | ONLINE

